Published in final edited form as:
*Channels (Austin)*. 2010 ; 4(3): 192–202.

# Rem GTPase Interacts with the Proximal $Ca_v1.2$ C-terminus and Modulates Calcium-dependent Channel Inactivation

**Chunyan Pang**, **Shawn M. Crump**[†], **Ling Jin**, **Robert N. Correll**, **Brian S. Finlin**, **Jonathan Satin**[†], and **Douglas A. Andres**[*]

[†]Department of Molecular and Cellular Biochemistry and Physiology, University of Kentucky College of Medicine, 741 South Limestone Street, Lexington, KY 40536-0509

## Abstract

The Rem, Rem2, Rad, and Gem/Kir (RGK) GTPases, comprise a subfamily of small Ras-related GTP-binding proteins, and have been shown to potently inhibit high voltage-activated $Ca^{2+}$ channel current following overexpression. Although the molecular mechanisms underlying RGK-mediated $Ca^{2+}$ channel regulation remains controversial, recent studies suggest that RGK proteins inhibit $Ca^{2+}$ channel currents at the plasma membrane in part by interactions with accessory channel β subunits. In this paper, we extend our understanding of the molecular determinants required for RGK-mediated channel regulation by demonstrating a direct interaction between Rem and the proximal C-terminus of $Ca_V1.2$ (PCT), including the CB/IQ domain known to contribute to $Ca^{2+}$/calmodulin (CaM)-mediated channel regulation. The Rem2 and Rad GTPases display similar patterns of PCT binding, suggesting that the $Ca_V1.2$ C-terminus represents a common binding partner for all RGK proteins. *In vitro* Rem:PCT binding is disrupted by $Ca^{2+}$/CaM, and this effect is not due to $Ca^{2+}$/CaM binding to the Rem C-terminus. In addition, co-overexpression of CaM partially relieves Rem-mediated L-type $Ca^{2+}$ channel inhibition and slows the kinetics of $Ca^{2+}$-dependent channel inactivation. Taken together, these results suggest that the association of Rem with the PCT represents a crucial molecular determinant in RGK-mediated $Ca^{2+}$ channel regulation and that the physiological function of the RGK GTPases must be reevaluated. Rather than serving as endogenous inhibitors of $Ca^{2+}$ channel activity, these studies indicate that RGK proteins may play a more nuanced role, regulating $Ca^{2+}$ currents via modulation of $Ca^{2+}$/CaM-mediated channel inactivation kinetics.

### Keywords

RGK GTPases; Ras; Calcium Channel; $Ca_V1.2$; Rem; Rem2; Rad; Gem; Calmodulin; Calcium-dependent inactivation

## INTRODUCTION

High voltage activated (HVA) $Ca^{2+}$ channels allow $Ca^{2+}$ influx upon membrane depolarization to regulate a wide variety of cellular functions including excitation-contraction coupling in muscle cells, neurotransmitter release and $Ca^{2+}$ transients in neurons, and hormone secretion in endocrine cells [1]. L-type $Ca^{2+}$ channels minimally consist of a pore-forming $\alpha_1$ subunit, an intracellular β subunit, and a transmembrane complex $\alpha_2/\delta$ [1], with each of the subunits contributing to the modulation of the kinetics and

[*]Address correspondence to: Dr. Douglas A. Andres, Department of Molecular and Cellular Biochemistry, University of Kentucky College of Medicine, BBSRB Room B179, 741 South Limestone Street, Lexington, KY 40536-0509, Tel: 859-257-6775, Fax: 859-323-1037, dandres@uky.edu.

voltage-dependence of channel gating properties [1, 2]. Intracellular domains of the pore-forming $\alpha_1$ subunit serve as scaffolds for the targeting and localization of a diverse array of regulatory molecules. A conserved $\alpha_1$ interaction domain (AID) located between the first and second repeats of the $Ca_v\alpha_1$-subunit (loop I–II), serves as a high affinity binding site for all $Ca^{2+}$ channel β subunits ($Ca_v\beta$) [3]. AID:$Ca_V\beta$ association promotes trafficking of channel complex to the plasma membrane and results in increased current densities [4–6]. The $Ca_V1.2$ C-terminus (CCT) serves as another major site of modulation. The L-type channel CCT (residues 1507–2171 for rabbit $Ca_V1.2$) is targeted by a variety of regulatory pathways, including PKA, PKC, CaM, CaMKII, and protein phosphatases PP1 and PP2A [1, 7, 8]. A conserved CB/IQ domain and regions proximal to the CB/IQ have been reported to contribute to channel auto-regulation, including $Ca^{2+}$–dependent inactivation (CDI) through $Ca^{2+}$-regulated interactions with calmodulin (CaM) [9]. $Ca^{2+}$ free CaM (ApoCaM) appears to be constitutively tethered to the $Ca_v1.2$ C-terminus [10–12], and a recent study by Pitt and colleagues suggests that $Ca^{2+}$ -bound CaM elicits a conformational change within the $Ca_v1.2$ C-terminus which promotes binding to the I–II intracellular linker, resulting in channel inactivation [13]. In skeletal and cardiac muscle cells, the distal C-terminus of L-type calcium channels is subject to proteolytic cleavage [14–16], and the released distal C-terminal fragment has been found to function as a potent autoinhibitory domain [17, 18]. This same liberated domain has been shown to traffic to the nucleus to modulate gene expression within neurons [19] and cardiac myocytes [20].

Rem, Rem2, Rad, and Gem/Kir (RGK) are members of a Ras-related GTPase subfamily with conserved structural and functional characteristics that distinguish them from other members of the Ras superfamily [21–26]. These include several substitutions within regions of the Ras GTPase core known to be involved in both GTP/GDP binding and hydrolysis, a conserved C-terminal extension that functions to direct membrane association [27–29] and serves as a regulatory domain [28, 30–35], and a large but structurally variable N-terminal domain [22, 36–38]. Uniquely, RGK proteins are expressed in a tissue- and cell-type dependent fashion, and are subject to complex transcriptional regulation [21, 23–26, 39].

RGK protein expression has been shown to potently inhibit high-voltage activated (HVA) $Ca^{2+}$ channel activity in both heterologous and native systems [26, 30, 31, 40–44], mediated in part through interactions with auxiliary β-subunits and a conserved domain within the RGK C-terminus that is required to direct plasma membrane trafficking [26, 28]. Although the mechanisms underlying RGK-mediated $Ca^{2+}$ channel regulation remain largely unknown, recent studies have suggested that plasma membrane-localized RGK proteins associate with the $Ca_V\alpha_1$ channel complex through $Ca_v\beta$ subunit binding [29, 41, 45]. Here, we expand upon the potential molecular mechanisms involved in RGK-mediated $Ca^{2+}$ channel regulation by identifying a direct interaction between Rem and the proximal C-terminus of $Ca_v1.2$(CCT) and provide evidence supporting a role for CCT association in Rem-dependent $Ca^{2+}$ channel regulation.

## RESULTS

### Rem interacts with the L-type, but not T-type $Ca_V\alpha_1$-CCT *in vitro*

Rem inhibits $I_{Ca,L}$ in part through association with auxiliary $Ca_V\beta$ subunits [28, 30, 40, 41, 43], but the contribution of the channel $\alpha_1$-subunit to Rem regulation remains poorly characterized [26]. To explore whether Rem interacts with the $Ca_v1.2$ C-terminus, tsA201 cells were transiently co-transfected with expression vectors encoding 3xFlag-tagged Rem and either 3xHA-empty vector (control), 3xHA-tagged full-length $Ca_v1.2$ C-terminus, or the indicated $Ca_v1.2$ C-terminal truncation mutants (Fig. 1A, B). HA-CCT or the CCT mutants were then isolated by immunoprecipitation, and bound Flag-Rem was visualized by immunoblotting. As seen in Fig. 1B, Rem was found to associate with full-length CCT

(CCT-FL) (Fig. 1B, *top panel*). This binding appears to involve interactions of Rem with both the proximal ($Ca_v1.2$ (1507–1669) (PCT)) and distal ($Ca_v1.2$ (1906–2171) (DCT)) domains, but not with the medial ($Ca_v1.2$ (1672–1905) (MCT)) portion of the $Ca_V1.2$-CCT (Fig. 1B, *top panel*). Although not all the CCT fragments were expressed at equivalent levels (Fig. 1C), MCT was highly expressed and immunoblotting confirmed that the transfected cells expressed similar levels of 3xFlag-Rem (Fig. 1B, *lower panel*).

RGK proteins are incapable of inhibiting T-type calcium channel function [30, 31], and the CCT domains of L- and T-type α-subunits display little overall sequence homology [46]. Therefore, as an added specificity control, we examined the interaction between Rem and the $Ca_V3.2$-CCT. Although the $Ca_v3.2$-CCT was expressed at greater levels than that of $Ca_v1.2$-CCT in tsA-201 cells (Fig. 1D, *bottom panel*), Rem failed to interact with $Ca_v3.2$-CCT (Fig. 1D, *top panel*). Taken together, these studies indicate that Rem interacts with both the proximal and distal portions of the L-type CCT, but not with the T-type CCT.

### *In vitro* association of RGK proteins with the proximal CCT

To further characterize the nature of the Rem-CCT association, we next used $^{35}S$-labeled, *in vitro* translated CCT fragments and recombinant glutathione-*S*-transferase (GST) fused Rem (GST-Rem) and GST-Rem-(1-265) to explore the Rem-CCT interaction. The generation of $^{35}S$-labeled CCT-FL or the other three CCT truncation mutants is shown in Figure 2A. GST-Rem directly bound $^{35}S$-labeled PCT (Fig. 2*B*, *top panel*), but failed to associate with MCT (Fig. 2*B*, *middle panel*). Interestingly, recombinant Rem also failed to interact with DCT (Fig. 2*B*, *bottom panel*) suggesting that Rem binding with the distal CCT may require additional cellular binding factors. Surprisingly, the conserved RGK C-terminus appears to contribute to CCT binding, since GST-Rem-(1-265) failed to associate with either CCT-FL or PCT (Fig. 2*C*). In addition, while previous work has suggested that RGK-mediated $Ca^{2+}$ channel regulation may be GTP-dependent [40, 44], both GDP-bound and GTPγS-bound Rem displaying equivalent *in vitro* PCT binding (Fig. 2*B*, *top panel*).

If CCT association is required for RGK-mediated channel regulation, we reasoned that CCT binding should be a common property for all RGK proteins. Importantly, when expressed in tsA201 cells, both Rem2 and Rad GTPases co-immunoprecipitate with the proximal and distal, but not the medial domain, of CCT (Figs. 3*A* and *B*). Thus, the ability to bind CCT is a conserved property for RGK family proteins and suggests that CCT association may contribute to RGK-mediated channel regulation.

### Rem-mediated $I_{Ca,L}$ inhibition does not require the distal CCT

To explore the contribution of the distal $Ca_V1.2$ C-terminus to Rem-dependent regulation of $Ca^{2+}$ channel current, we examined the modulation of $Ca_V1.2$(1–1905), a deletion mutant lacking the final 265 residues of the C-terminus. Co-expression of $Ca_V1.2$(1–1905) with $Ca_Vβ1b$+GFP in tsA201 cells resulted in appreciable whole cell currents (−12.0 + 4.4 pA/pF, *filled squares*, n=4) (Fig. 3C). Importantly, expression of wild-type GFP-Rem resulted in a potent reduction in ionic current expression (−0.3 + 0.3 pA/pF, *open circles*, n=5), which is similar to the inhibition observed with full-length $Ca_V1.2$+$Ca_Vβ1b$ (see Fig. 4D). Similar results were obtained using $Ca_V1.2$(1–1905)+$Ca_Vβ2a$ (data not shown), suggesting that the C-terminus of $Ca_V1.2$ distal to position 1905 does not contribute to Rem-mediated regulation of $Ca^{2+}$ channel current.

### Plasma membrane targeting contributes to Rem:CCT association

The RGK C-terminus appears to play important roles in both plasma membrane targeting and $Ca^{2+}$ channel regulation [26]. To examine the importance of this domain in CCT binding, we analyzed the interaction of wild-type Rem and Rem-(1-265) with PCT using co-

immunoprecipitation from tsA201 cell lysates. The Rem-(1-265) truncation mutant lacks the conserved RGK C-terminus, is not localized at the plasma membrane, and does not alter $Ca^{2+}$ channel current expression [28, 30]. Consistent with the binding studies in Figure 2*C*, Rem-(1-265) failed to associate with HA-PCT, whereas full-length Rem displayed PCT binding (Fig. 4*A*). We next investigated whether the Rem C-terminus directly contributed to CCT binding. For these studies, we made use of two chimeric proteins in which the C-terminus of K-Ras4B and H-Ras were fused to Rem-(1-265) [28]. Addition of either plasma membrane trafficking motif has been found to restore both membrane localization and $Ca^{2+}$ channel regulation [28], and co-immunoprecipitation analysis found that both chimeric proteins are capable of PCT binding (Fig. 4*A*). Therefore, Rem:CCT association is correlated with both Rem-mediated $Ca^{2+}$ channel regulation and plasma membrane localization. As an added specificity control, Rem-(1-265)-HSAAX (mutation of the CAAX motif cysteine to serine) was generated. Mutation of the CAAX motif cysteine disrupts protein farnesylation 47–49 and confocal microscopy confirms that Rem-(1-265)-HSAAX is not localized to the plasma membrane (Supplemental Fig. S1). Co-immunoprecipitation analysis found that Rem-(1-265)-HSAAX does not associate with CCT-FL (Fig. 4*B*) but retains $Ca_V\beta_{1b}$ subunit binding (Fig. 4*C*). While GFP-Rem-(1-265)-HCAAX expression resulted in a potent reduction in ionic current expression (−1.1 ± 0.3 pA/pF, *closed triangles*, n=8) when co-expressed with $Ca_V1.2+\beta_{1b}$ in tsA201 cells (Fig. 4*D*), GFP-Rem-(1-265)-HSAAX did not significantly alter either current density or voltage-dependent channel gating properties (Fig. 4*D*). Whole cell currents elicited in the presence of $Ca_V1.2+\beta_{1b}$+GFP-Rem-(1-265)-HSAAX (−17.7 ± 3.9 pA/pF, *filled squares*, n=9) were indistinguishable from control currents in cells expressing $Ca_V1.2+\beta_{1b}$+GFP (−18.5 ± 4.7 pA/pF, *open circles*, n=10) (Fig. 4*D*). As a final specificity control, co-immunoprecipitation analysis found that the isolated Rem C-terminus (residues 266–297) does not directly associate with PCT (Fig. 4E). Taken together, these data suggest that plasma membrane localization, but not sequences within the C-terminus of Rem, contribute to Rem:CCT association and support the notion that CCT binding is necessary for effective Rem-mediated channel regulation.

## $Ca^{2+}$-calmodulin inhibits Rem:CCT binding

Since calmodulin (CaM) is known to interact with the $Ca_V1$ C-terminus in the same region required for Rem association [9] (Figs. 1*B* and 2*B*), and also associates with the C-terminus of Rem [28, 35, 50], we next examined whether CaM binding might regulate Rem:CCT association. Compared to GST-Rem:CCT-FL binding in the presence of EGTA, CCT-FL binding was modestly decreased by the addition of 2 mM $Ca^{2+}$ (Fig. 5*A*, *top panel*, compare lanes 2 and 4). However, while the addition of CaM to the *in vitro* binding reaction had no obvious effect on Rem:CCT-FL association in the presence of EGTA, the interaction between Rem and CCT-FL was almost completely inhibited upon the addition of $Ca^{2+}$/CaM (Fig. 5*A*, *top panel*, compare lanes 6 and 8). Similar results were seen using recombinant GST-Rem and PCT (Fig. 5*A*, *bottom panel*). Addition of high concentrations of $Ca^{2+}$ also disrupted Rem:PCT association in TsA201 cell lysates. As seen in Figure 5*B*, Rem displayed PCT binding in lysis buffer containing EGTA but Rem/PCT association was abolished in the presence of excess $Ca^{2+}$ (Fig. 5*B*, *top panel*, compare lanes 1 and 2). Transfected cells expressed similar levels of Rem (Fig. 5*B*, *bottom panel*) and PCT (Fig. 5*B*, *middle panel*), indicating that the loss of binding was not the result of $Ca^{2+}$-dependent proteolysis or a transfection artifact. The addition of exogenous CaM did not further alter the relative binding affinity between Rem and PCT either in the presence of $Ca^{2+}$ or EGTA (data not shown). Taken together, these data suggest that $Ca^{2+}$/CaM acts to inhibit Rem and PCT association.

### $Ca^{2+}$/CaM-mediated inhibition of Rem:PCT association is not due to CaM binding to the Rem C-terminus

To determine whether CaM binding to Rem disrupts Rem:CCT association, we examined the effect of CaM on PCT binding to Rem-(1-265)-KCAAX and Rem-(1-265)-HCAAX [28]. Whereas the K-Ras4B-CAAX motif shares several properties with the Rem C-terminus, including a polybasic domain capable of PIP lipid-mediated plasma membrane targeting and CaM association [27, 51, 52], the H-Ras-CAAX domain contains a prenylation/palmitoylation membrane localization signal and does not bind CaM [51]. CaM sepharose pulldown assays were used to confirm these properties. As expected, only WT-Rem and Rem-(1-265)-KCAAX displayed CaM binding (Fig. 5*C*). Furthermore, both Rem-(1-265)-KCAAX and Rem-(1-265)-HCAAX bound PCT in the absence, but not the presence of excess $Ca^{2+}$ in the immunoprecipitation assay (Fig. 5*B*). These data indicate that the $Ca^{2+}$/CaM mediated blockade of Rem:PCT association does not involve direct CaM binding to the Rem C-terminus.

### Overexpression of CaM partially blocks Rem-mediated $I_{Ca,L}$ inhibition

Since association of Rem with the $Ca_V1.2$ C-terminus appears to play a role in the blockade of $I_{Ca,L}$ (Fig. 4*D*) and $Ca^{2+}$/CaM inhibits *in vitro* Rem:PCT association (Figs. 5*A*, *B*), we reasoned that CaM may serve to modulate Rem-mediated $Ca^{2+}$ channel blockade. Peak currents elicited from tsA201 cells expressing $Ca_v1.2$+Flag-$\beta_{2a}$+GFP+HA-CaM (Fig. 6*A*, *filled squares*, −18.6±6.1 pA/pF, n=11) using 30 mM $Ba^{2+}$ as the charge carrier were not significantly different from those obtained in the absence of co-expressed CaM [$Ca_v1.2$+Flag-$\beta_{2a}$+GFP+pKH3] (Fig. 6*A*, *open diamonds*, −12.3±2.4 pA/pF, n=11). As expected, co-expression of GFP-Rem was capable of generating complete current blockade in the presence of 30 mM $Ba^{2+}$ (Fig. 6*A*, *open circles*, −0.3±0.4 pA/pF, n=6). However, co-expression of HA-CaM was able to partially relieve Rem-mediated blockade of L-type ionic current (Fig. 6*A*, *C*). In these experiments, CaM overexpression resulted in peak current densities of >3.5 pA/pF (Fig. 6*A*, *filled triangles*, −3.6±1.2 pA/pF, n=12 and Fig. 6*C*), which is ~19% of the peak current density elicited in the absence of Rem overexpression. Although the average peak current densities generated from $Ca_v1.2$+Flag-$\beta_{2a}$+GFP-Rem+pKH3 and $Ca_v1.2$+Flag-$\beta_{2a}$+GFP-Rem+HA-CaM transfection were not found to be statistically different, 7 out of 12 cells expressing Rem and CaM generated detectable ionic current while only 1 out of 6 cells transfected with $Ca_v1.2$+Flag-$\beta_{2a}$+GFP-Rem+pKH3 generated any detectable ionic current (peak current density of the single cell = −2.3 pA/pF). We next tested the effect of HA-tagged CaM overexpression on Rem-mediated channel inhibition using 30 mM $Ca^{2+}$ as the charge carrier. Peak current density elicited from cells expressing $Ca_v1.2$+Flag-$\beta_{2a}$+GFP+HA-CaM (Fig. 6*B*, *filled squares*, −6.9±1.6 pA/pF, n=20 and Fig. 6D) was not statistically different from those seen following expression of $Ca_v1.2$+Flag-$\beta_{2a}$+GFP+pKH3 (Fig. 6*B*, *open diamonds*, −6.3±1.9 PA/pF, n=11, and Fig. 6*D*). As expected, Rem expression resulted in a complete blockade of current expression in this system (Fig. 6*B*, *open circles*, −0.1±0.2 pA/pF, n=8, and Fig. 6*D*). However, co-expression of Rem and CaM resulted in >3 pA/pF peak inward current (Fig. 6*B*, *filled triangles*, −3.0±0.7 pA/pF, n=16, and Fig. 6*D*), which was significantly different from the average current density elicited from the $Ca_v1.2$+Flag-$\beta_{2a}$+GFP-Rem+pKH3 transfection (Fig. 6*D*) ($p<0.01$). CaM co-expression resulted in a partial restoration of $I_{Ca,L}$ (43% of the peak current elicited in 30 mM $Ca^{2+}$ in the absence of Rem) (Fig. 6*B* and 6*D*). Immunoblotting of whole cell lysates indicate that overexpression of CaM does not alter the expression of Rem or channel subunits (Supplemental Fig. S2). Together these data indicate that CaM overexpression partially antagonizes Rem-mediated $Ca^{2+}$ channel current inhibition.

### Rem alters the kinetics of calcium-dependent channel inactivation

It is well established that CaM bound to the $Ca_V1$ C-terminus plays a critical role in the generation of calcium dependent inactivation [9]. Because Rem interacts with PCT and overexpression of CaM partially relieves Rem-mediated L-type $Ca^{2+}$ channel inhibition (Fig. 6A, B), we next asked whether Rem alters the kinetics of voltage-dependent inactivation (VDI) or calcium-dependent inactivation (CDI). Fig. 7A shows the superimposed representative time course of the $I_{Ba}$ generated during 300 ms test pulses to +5 mV from Vh=−80 mV (holding potential) from the indicated transfection experiments; all of the current traces were normalized in order to facilitate the kinetics comparison. The $Ba^{2+}$-current restored by CaM overexpression had decay kinetics with the same time course as those observed in the absence of Rem expression (Fig. 7*A*). The degree of VDI was analyzed using $r_{600}$, the ratio of the residual current at 600 ms to the initial peak. At 600 ms after the onset of the depolarization, ~70% of the peak current remains for Cav1.2+Flag-$\beta_{2a}$+GFP+pKH3 transfection, and the co-expression of either CaM or Rem/CaM did not affect VDI kinetics (Fig. 7*C*). Figure 7*B* shows the superimposed representative time course of the $I_{Ca}$ generated during initial 300 ms of test pulses to +20 mV from $V_h$= −80 mV from the indicated transfection experiments. When compared to wild-type L-type $Ca^{2+}$ channels, or channels in the presence of exogenous CaM, Rem and CaM co-expression was found to significantly slow current decay (Fig. 7*B*). In order to quantitate the affect of Rem/CaM expression on CDI, the time constants of inactivation (tau) were derived from individual current traces (see “Materials and Methods” for details). As seen in Figure 7*D*, CaM expression did not alter inactivation kinetics for the $Ca_V1.2$+Flag-$\beta_{2a}$ channel in the depolarizing potentials from 0 mV to 40 mV, which is consistent with previous studies [12, 53]. However, inactivation kinetics following overexpression of $Ca_v1.2$+Flag-$\beta_{2a}$+GFP-Rem +HA-CaM displayed a statistically significant difference at depolarizing potentials ranging from 0 mV to 30 mV (* $P<0.05$; ** $P<10^{-4}$). Indeed, the average $tau_{fast}$ value increased following Rem and CaM co-expression (Fig. 7*D*, *filled circles*, 63.59±4.49 ms, n=8) by 64% when compared with cells expressing CaM alone (Fig. 7*D*, *open squares*, 38.83±2.11 ms, n=12) at 20 mV, which is the depolarizing potential corresponding to the peak current. The average peak current density resulting from the overexpression of Rem+CaM is about 43% of the peak current elicited in the absence of Rem. Given that CDI is dependent on $Ca^{2+}$-entry we were concerned that the apparent loss of CDI with Rem+CaM co-expression simply was secondary to a decreased absolute degree of $Ca^{2+}$-entry. To evaluate this possibility, we plotted the macroscopic decay time constant $tau_{fast}$ against the peak $I_{Ca,L}$ density measured at +20 mV from individual cells in the presence or absence of Rem. Macroscopic $I_{Ca,L}$ decay was slower for Rem+CaM compared to CaM overexpression even in fortuitous instances of similar $I_{Ca,L}$ density (Supplemental Fig. S3). These data suggest that Rem significantly slows the kinetics of CDI.

## DISCUSSION

All members of RGK GTPases have been found to act as potent inhibitors of high-voltage activated (HVA) $Ca^{2+}$ channel function when overexpressed [26, 30, 31, 33–35, 39–44]. While binding to accessory $Ca_V\beta$ subunits contributes to RGK-mediated HVA $Ca^{2+}$-channel regulation [30, 40–44], this interaction alone is not sufficient for Rem-dependent current blockade [28, 54]. In the present study, we provide new insight into the mechanisms of RGK-mediated $Ca^{2+}$ channel regulation through the identification of an interaction between the $Ca_V1.2$-CCT and RGK GTPases and find that Rem:CCT association appears to contribute to Rem-dependent regulation of L-type $Ca^{2+}$ channel activity. $Ca^{2+}$/CaM is able to disrupt Rem:CCT binding *in vitro* (Fig. 5A) and overexpression of CaM partially reverses Rem-mediated VDCC inhibition (Fig. 6). Finally, the Rem:CCT interaction site is implicated in CDI because Rem - CaM co-expression was found to significantly alter the kinetics of CDI (Fig. 7*B*, *D*). Based upon these findings we propose that RGK proteins can associate with

Cavβ and CCT, and that these interactions promote reorganization of $Ca_V\alpha_1$ intracellular domains to generate the blockade of current expression which is the hallmark of RGK-dependent $Ca^{2+}$-channel regulation upon overexpression [26, 30, 31, 33–35, 39–44]. Our studies also pointed out the possibility that Rem may function as an endogenous regulator for $Ca^{2+}$/CaM-mediated channel inactivation.

The L-type $Ca^{2+}$-channel exists in most cells as a multi-protein complex. Although heterologous expression studies have led to great insight into $Ca^{2+}$-channel function, over-expression studies increase selected components of the channel complex and must be cautiously interpreted. For example, the bulk of RGK – $Ca^{2+}$-channel studies never over-express CaM, yet CaM is known to be an integral component of the L-type channel complex [10–12] and even without CaM over-expression, CDI occurs. The observation of CDI led us and others to conclude that endogenous (in this case tsA201 cell) CaM is sufficiently abundant to modulate $I_{Ca,L}$. However, this assumes that the overexpressed protein does not compete with CaM for access to the $Ca^{2+}$-channel complex. A second reason we previously overlooked CaM co-expression was that based on Western blotting CaM abundance was relatively high in tsA201 cells. This overlooks the important finding that CaM has numerous interacting proteins in a cell. Taken together, our data now suggest that RGK proteins via interactions with $Ca_V1.2$ proximal C-terminus effectively compete with CaM. Although, CaM is not limiting for $I_{Ca,L}$ carried by $Ca_V1.2$ ($+Ca_V\beta_{2a}$) expression, the presence of excess Rem reveals the limiting nature of endogenous CaM. This new interpretation logically leads to a provocative suggestion – that a function of RGK proteins is to not only govern $I_{Ca,L}$, but also to influence CaM-channel regulation.

Our studies indicate that Rem overexpression only partially inhibits $Ca^{2+}$ current amplitude in the presence of overexpressed CaM (Fig. 6*A*, *B*), and that co-expression of CaM and Rem slows the inactivation kinetics of CDI (Fig. 7*B*, *D*). Altering CDI has a strong effect on action potential duration in cardiac myocytes [55]. These data suggest that RGK proteins may serve to increase $Ca^{2+}$ flux under physiological conditions. Moreover, the complete channel blockade observed in earlier studies may be an artifact of *in vitro* overexpression resulting from a cellular imbalance between Rem and CaM. These results also address a vexing issue in RGK signaling- namely if RGK proteins potently inhibit $Ca^{2+}$ channel function, and endogenous RGK proteins are expressed in excitatory cells, why are L-type $Ca^{2+}$ currents maintained? These data indicate that rather than serving as endogenous inhibitors of $Ca^{2+}$ channel activity, RGK proteins may play a more nuanced role, regulating $Ca^{2+}$ currents via modulation of $Ca^{2+}$/CaM-mediated channel inactivation kinetics. It has been reported that levels of Rad mRNA and protein are decreased significantly in failing human hearts and that Rad expression is decreased significantly in murine cardiac hypertrophy models [56], suggesting that Rad may play an important role in maintaining normal cardiac function. However, whether endogenous L-type $Ca^{2+}$ channel function is modified, the kinetics of CDI are changed, or action potential duration is altered in the cardiomyocytes of Rad knockout animals has not yet been examined. A careful examination of these issues in Rad knockout myocytes, or the generation and analysis of additional RGK knockout animal models, will be needed to fully address these important questions.

Rem, Rad, and Rem2 are each capable of interacting with both the proximal (residues 1507–1669) and the distal (residues 1906–2171) domains of the $Ca_V1.2$-CCT when co-overexpressed in tsA201 cells (Figs. 1, 3). However, *in vitro* binding studies indicate that the interaction with PCT is direct, while that with the DCT domain is indirect and may require additional intracellular anchoring proteins (Fig. 2*B*). Interestingly, the proximal CCT contains several functionally important domains including the conserved EF-hand, A, CB and IQ domains, all of which have established regulatory roles in L-type $Ca^{2+}$ channel function. In particular, the A, CB and IQ domains have been reported to serve as docking

sites for both apocalmodulin (ApoCaM) and $Ca^{2+}$-CaM [9]. Although the identity of the exact binding sites for ApoCaM and $Ca^{2+}$-CaM on the CCT remain controversial, and appears to depend upon the functional status of the particular channel under study [9], it has been proposed that $Ca^{2+}$ binding to CaM elicits a major conformational change in the CCT which initiates CDI [13, 57]. Our studies indicate that $Ca^{2+}$/CaM inhibits Rem:CCT association *in vitro* (Fig. 5*A*), suggesting that Rem and CaM could compete for interaction with the proximal CCT domain, either by targeting overlapping docking sites within the PCT, or by having $Ca^{2+}$/CaM-mediated conformational rearrangements of the PCT disrupt Rem association. In this model, bound Rem would present a barrier to $Ca^{2+}$/CaM-mediated conformational rearrangement of the PCT, and displacement of Rem would slow the $Ca^{2+}$/CaM-mediated structural reorganization of the $Ca_V1.2$ C-terminus which results in CDI. Studies are underway to examine whether A, CB and /or IQ domains are involved in the direct association with Rem.

In summary, we demonstrate that RGK proteins interact with two distinct domains within the $Ca_V1.2$-CCT, including a direct interaction with the proximal C-terminus. Furthermore, while plasma membrane localization appears to promote both Rem:CCT association and $Ca^{2+}$ channel regulation, it is dispensable for β subunit binding, supporting an important role for Rem:PCT interaction in Rem-mediated $Ca^{2+}$ channel regulation. Moreover, there is an interplay between $Ca^{2+}$/CaM:PCT association and Rem:PCT association which appears capable of modulating $Ca^{2+}$/CaM-mediated CDI kinetics. Additional studies will be needed to identify the cellular signaling pathways that control Rem-mediated $Ca^{2+}$ channel activity and to characterize the interplay between Rem:CCT and Rem:$Ca_v\beta$ binding in $Ca^{2+}$ channel regulation.

## MATERIALS AND METHODS

### Protein expression

Mammalian expression vectors for $Ca_v1.2$, Flag-$\beta_{2a}$, and Flag-$\beta_{1b}$ subunits have been described previously [30]. GFP-$Ca_v1.2$ (rabbit) was kindly provided by K. Beam (University of Colorado Health and Sciences Center, Aurora, CO). Truncation mutants for $Ca_V1.2$ were generated using the Quick change site-directed mutagenesis kit (Stratagene, La Jolla, CA), while Rem(266–297) was generated by PCR. Rem containing a CAAX box have been described previously, and the SAAX mutants produced by mutagenesis [28]. Full length and truncated $Ca_V1.2$-CCT cDNAs were subcloned into pCite4 (Novagen) for production of *in vitro* translated proteins. pKH3-mCaM was kindly provided by Dr. Daniel Noonan (Dept. of Biochemistry, Univ. of Kentucky). All site-directed mutants and PCR reaction products were verified by DNA sequencing.

### In vitro GST pulldown assay

GST-Rem and GST-Rem(1-265) were produced as described previously [21]. Radiolabeled proteins were prepared by *in vitro* transcription and translation in the presence of [$^{35}$S] methionine using the Single Tube Protein System 3 (STP3) kit (Novagen). Binding of radiolabeled CCT to Rem was assessed as follows. Glutathione-Sepharose beads (GE Healthcare) (10 µl) were resuspended in EDTA buffer (50 mM Tris, pH 7.5, 100 mM NaCl, 0.05% Tween 20, 1 mM DTT, 1 mM EDTA), and GST or GST-Rem (10 µg) added. The beads were incubated for 5 min with end-over-end rotation at 4 °C, washed with ice-cold EDTA buffer (1 ml), and then with either ice-cold EDTA buffer (1 ml), GDP buffer (1 ml) (50 mM Tris, pH 7.5, 100 mM NaCl, 0.05% Tween 20, 1 mM DTT, 10 mM $MgCl_2$, 20 µM GDP), or GTP buffer (GDP buffer with 20 µM GTPγS) (1 ml) to promote nucleotide exchange. Binding was initiated by the addition of $^{35}$[S]-labeled CCT protein (4 µl) and incubated for 3 h at 4 °C with end-over-end rotation (100 µl total volume). Resin was

washed three times and bound fraction eluted using assay buffer containing 25 mM glutathione (40 µl total). Fractions were resolved on 10% SDS-PAGE gels, the gels dried and exposed to film for 16–72 h. Purified bovine CaM protein was kindly provided by Dr. Thomas Vanaman (Dept. of Biochemistry, Univ. of Kentucky.

### Co-immunoprecipitation analysis

Expression vectors expressing $Ca_V1.2$, RGK GTPases, or various mutants, were co-transfected into tsA201 cells by the calcium phosphate method [58]. Forty-eight hours post-transfection, cells were suspended in ice-cold immunoprecipitation (IP) buffer [20 mM Tris, pH 7.5, 250 mM NaCl, 1% TX-100, 0.5 mM DTT, 1× protease inhibitor mixture (Calbiochem), 10 mM $MgCl_2$, 10 µM GTPγS], lysed by sonication, subjected to centrifugation (100,000 × *g*), and 0.5 mg of the cleared supernatant incubated with Protein G Sepharose (12.5 µl) (Pharmacia) and anti-HA antibody (5 µg) for 3 h with rotation at 4°C (500 µl total volume). The beads were pelleted and washed three times with IP buffer (1 ml). Fractions were resolved on SDS/PAGE, transferred to nitrocellulose, and subjected to immunoblot analysis using biotinylated-Flag antibody (1 µg/ml) and streptavidin–horseradish peroxidase (Pierce) (1:40,000 dilution). Expression of recombinant proteins was examined by immunoblotting using either anti-Flag (Sigma) or anti-HA monoclonal antibodies (1 µg/ml).

### Confocal imaging

Confocal imaging of green fluorescent protein (GFP)-tagged Rem protein was performed as previously described [42]. Images displayed are representative of the cells observed.

### β Subunit Association Assay

Co-immunoprecipitation of Rem with Flag-$Ca_V\beta_{1b}$ in tsA201 cells was performed as previously described [30, 59].

### Calmodulin binding assay

TsA201 cells were transfected with Rem, Rem-(1-265), Rem-(1-265)-KCAAX, Rem-(1-265)-HCAAX or empty p3xFlag-CMV10 using the calcium phosphate method 58. 48 h post-transfection, cells were harvested and binding of Rem or Rem chimeric proteins to calmodulin was performed as previously described 28. The eluted proteins were resolved on 10% SDS-PAGE, transferred to nitrocellulose and immunoblotted with anti-Flag M2 monoclonal antibody (1 µg/ml) (Sigma) to detect bound Rem.

### Electrophysiology

TsA201 cells were transfected with the indicated plasmids using the calcium phosphate method, and whole-cell patch clamp experiments were performed as described previously [28, 59]. Transfected cells were identified by GFP expression. The selection of $Ca_V\beta$ subunit was motivated by the desire to compare results in the present study with our earlier work (28), while studies exploring CDI used $Ca_V\beta2a$ because of the larger current densities generated. The whole cell configuration of the patch-clamp technique was used to measure ionic current. Patch electrodes with resistances of 1–2 mΩ contained (in mM) 150 CsCl, 3 EGTA, 1 $MgCl_2$, 5 Mg-ATP, and 5 HEPES, pH 7.36. The bath solution consisted of (in mM) 112.5 CsCl, 30 $BaCl_2$ or $CaCl_2$, 1 $MgCl_2$, 10 tetraethylammonium chloride, 5 glucose, 5 HEPES, PH 7.4. The I–V relationship was determined by applying 1000 ms voltage pulses at 0.25 Hz to potentials between −90 and 80 mV in 5 mV increments from a holding potential of −80 mV. Signals were amplified with an Axopatch 200B amplifier and 333 kHz A/D system (Axon Instruments, Union City, CA). All recordings were performed at room temperature (20–22°C). Data was analyzed with Clampfit 9 (Axon Instruments) software. In

Fig. 6C and Fig. 6D, values are reported as normalized mean at 5 mV ± SE for $Ba^{2+}$ currents and as normalized mean at 20 mV ± SE for $Ca^{2+}$ currents, and significance was determined using Kruskal-Wallis test followed by a *post hoc* Dunn's test with p-values of <0.01 (Graphpad prism5). For the data analysis in Fig. 7C, the degree of voltage-dependent inactivation was analyzed using $r_{600}$, the ratio of the residual current values at 600 ms and at the initial peak. For the data analysis shown in Fig. 7D, $Ca^{2+}$ currents recorded during a typical 1000 ms test pulse applied ranging from 0 mV to +40 mV from a holding potential of −80 mV at indicated experimental conditions were analyzed using pclamp10 software and the time constants of inactivation were derived from fitting the decay phases of the time courses with the following biexponential function equation: $i(t) = A1 * \exp(-t/Tau_{fast}) + A2 * \exp(-t/Tau_{slow}) + C$, where $t$ is the time; $A1$, $A2$, $Tau_{fast}$, and $Tau_{slow}$ are the amplitudes and time constants of the fast or slow exponential components; and $C$ is the fraction of noninactivating current. The fast component of inactivation was used for the analysis of $Ca^{2+}$-dependent channel inactivation. For the data analysis shown in Fig. 7D, statistical significance was determined using student's t-test (OriginLab, Northampton, MA) denoted by single (P<0.05) or double (P<0.00005) asterisks.

## Supplementary Material

Refer to Web version on PubMed Central for supplementary material.

## Acknowledgments

We wish to thank Dr. Carole Moncman for her assistance with the confocal imaging studies and members of the Andres lab for critical reading of this manuscript. This work was supported by Public Health Service Grants HL072936 (to DAA), HL074091 (to JS), and P20 RR20171 from the National Center for Research Resources, National Institutes of Health (to DAA), an American Diabetes Junior Faculty Award 7-05-JF-16 to (BSF), and an American Heart Association pre-doctoral fellowship and an NIH Interdisciplinary Cardiovascular Training Grant T32 HL072743 (to RNC).

## The abbreviations used are

| | |
|---|---|
| **RGK** | Rem, Rem2, Rad, and Gem/Kir GTPase |
| **CCT** | $Ca_V\alpha_1$ C-terminus |
| **VDCC** | voltage-dependent calcium channel |
| **VDCC** | alpha subunit ($Ca_V\alpha$) |
| **VDCC** | beta subunit ($Ca_V\beta$) |
| **HVA** | high-voltage activated |
| **AID** | $Ca_V\alpha_1$ loop I–II interaction domain |
| **CDI** | calcium-dependent inactivation |
| **VDI** | voltage-dependent inactivation |
| **PIP** | phosphorylated phosphatidylinositide lipids |
| **GST** | glutathione-*S*-transferase |
| **GFP** | green fluorescent protein |
| **HA** | hemagglutinin |
| **PKA** | protein kinase A |
| **PKC** | protein kinase C |

| | |
|---|---|
| **CaM** | calmodulin |
| **CaMKII** | calmodulin kinase II |
| **PP1** | protein phosphatase 1 |
| **PP2A** | protein phosphatase 2A |

## REFERENCES


1. Catterall WA. Structure and regulation of voltage-gated Ca2+ channels. Annu Rev Cell Dev Biol. 2000; 16:521–555. [PubMed: 11031246]
2. Walker D, De Waard M. Subunit interaction sites in voltage-dependent Ca2+ channels: role in channel function. Trends Neurosci. 1998; 21:148–154. [PubMed: 9554724]
3. Pragnell M, De Waard M, Mori Y, Tanabe T, Snutch TP, Campbell KP. Calcium channel beta-subunit binds to a conserved motif in the I–II cytoplasmic linker of the alpha 1-subunit. Nature. 1994; 368:67–70. [PubMed: 7509046]
4. Richards MW, Butcher AJ, Dolphin AC. Ca2+ channel beta-subunits: structural insights AID our understanding. Trends Pharmacol Sci. 2004; 25:626–632. [PubMed: 15530640]
5. Bichet D, Cornet V, Geib S, Carlier E, Volsen S, Hoshi T, et al. The I–II loop of the Ca2+ channel alpha1 subunit contains an endoplasmic reticulum retention signal antagonized by the beta subunit. Neuron. 2000; 25:177–190. [PubMed: 10707982]
6. Dolphin AC. Beta subunits of voltage-gated calcium channels. J Bioenerg Biomembr. 2003; 35:599–620. [PubMed: 15000522]
7. Kamp TJ, Hell JW. Regulation of cardiac L-type calcium channels by protein kinase A and protein kinase C. Circulation research. 2000; 87:1095–1102. [PubMed: 11110765]
8. Pitt GS. Calmodulin and CaMKII as molecular switches for cardiac ion channels. Cardiovasc Res. 2007; 73:641–647. [PubMed: 17137569]
9. Halling DB, Aracena-Parks P, Hamilton SL. Regulation of voltage-gated Ca2+ channels by calmodulin. Sci STKE. 2006; 2006:er1. [PubMed: 16685765]
10. Erickson MG, Alseikhan BA, Peterson BZ, Yue DT. Preassociation of calmodulin with voltage-gated Ca(2+) channels revealed by FRET in single living cells. Neuron. 2001; 31:973–985. [PubMed: 11580897]
11. Zuhlke RD, Pitt GS, Deisseroth K, Tsien RW, Reuter H. Calmodulin supports both inactivation and facilitation of L-type calcium channels. Nature. 1999; 399:159–162. [PubMed: 10335846]
12. Peterson BZ, DeMaria CD, Adelman JP, Yue DT. Calmodulin is the Ca2+ sensor for Ca2+ -dependent inactivation of L-type calcium channels. Neuron. 1999; 22:549–558. [PubMed: 10197534]
13. Kim J, Ghosh S, Nunziato DA, Pitt GS. Identification of the components controlling inactivation of voltage-gated Ca2+ channels. Neuron. 2004; 41:745–754. [PubMed: 15003174]
14. Brawley RM, Hosey MM. Identification of two distinct proteins that are immunologically related to the alpha 1 subunit of the skeletal muscle dihydropyridine-sensitive calcium channel. J Biol Chem. 1992; 267:18218–18223. [PubMed: 1325462]
15. Gao T, Puri TS, Gerhardstein BL, Chien AJ, Green RD, Hosey MM. Identification and subcellular localization of the subunits of L-type calcium channels and adenylyl cyclase in cardiac myocytes. J Biol Chem. 1997; 272:19401–19407. [PubMed: 9235939]
16. De Jongh KS, Warner C, Colvin AA, Catterall WA. Characterization of the two size forms of the alpha 1 subunit of skeletal muscle L-type calcium channels. Proceedings of the National Academy of Sciences of the United States of America. 1991; 88:10778–10782. [PubMed: 1720551]
17. Hulme JT, Yarov-Yarovoy V, Lin TW, Scheuer T, Catterall WA. Autoinhibitory control of the CaV1.2 channel by its proteolytically processed distal C-terminal domain. J Physiol. 2006; 576:87–102. [PubMed: 16809371]
18. Gao T, Cuadra AE, Ma H, Bunemann M, Gerhardstein BL, Cheng T, et al. C-terminal fragments of the alpha 1C (CaV1.2) subunit associate with and regulate L-type calcium channels containing C-

terminal-truncated alpha 1C subunits. J Biol Chem. 2001; 276:21089–21097. [PubMed: 11274161]

19. Gomez-Ospina N, Tsuruta F, Barreto-Chang O, Hu L, Dolmetsch R. The C terminus of the L-type voltage-gated calcium channel Ca(V)1.2 encodes a transcription factor. Cell. 2006; 127:591–606. [PubMed: 17081980]
20. Schroder E, Byse M, Satin J. L-type calcium channel C terminus autoregulates transcription. Circulation research. 2009; 104:1373–1381. [PubMed: 19461046]
21. Finlin BS, Andres DA. Rem is a new member of the Rad- and Gem/Kir Ras-related GTP-binding protein family repressed by lipopolysaccharide stimulation. J Biol Chem. 1997; 272:21982–21988. [PubMed: 9268335]
22. Finlin BS, Shao H, Kadono-Okuda K, Guo N, Andres DA. Rem2, a new member of the Rem/Rad/Gem/Kir family of Ras-related GTPases. Biochem J. 2000; 347(Pt 1):223–231. [PubMed: 10727423]
23. Cohen L, Mohr R, Chen YY, Huang M, Kato R, Dorin D, et al. Transcriptional activation of a ras-like gene (kir) by oncogenic tyrosine kinases. Proc Natl Acad Sci U S A. 1994; 91:12448–12452. [PubMed: 7809057]
24. Maguire J, Santoro T, Jensen P, Siebenlist U, Yewdell J, Kelly K. Gem: an induced, immediate early protein belonging to the Ras family. Science. 1994; 265:241–244. [PubMed: 7912851]
25. Reynet C, Kahn CR. Rad: a member of the Ras family overexpressed in muscle of type II diabetic humans. Science. 1993; 262:1441–1444. [PubMed: 8248782]
26. Correll RN, Pang C, Niedowicz DM, Finlin BS, Andres DA. The RGK family of GTP-binding proteins: Regulators of voltage-dependent calcium channels and cytoskeleton remodeling. Cell Signal. 2008; 20:292–300. [PubMed: 18042346]
27. Heo WD, Inoue T, Park WS, Kim ML, Park BO, Wandless TJ, et al. PI(3,4,5)P3 and PI(4,5)P2 lipids target proteins with polybasic clusters to the plasma membrane. Science. 2006; 314:1458–1461. [PubMed: 17095657]
28. Correll RN, Pang C, Finlin BS, Dailey AM, Satin J, Andres DA. Plasma membrane targeting is essential for Rem-mediated Ca2+ channel inhibition. J Biol Chem. 2007; 282:28431–28440. [PubMed: 17686775]
29. Correll RN, Botzet GJ, Satin J, Andres DA, Finlin BS. Analysis of the Rem2 - voltage dependant calcium channel beta subunit interaction and Rem2 interaction with phosphorylated phosphatidylinositide lipids. Cell Signal. 2008; 20:400–408. [PubMed: 18068949]
30. Finlin BS, Crump SM, Satin J, Andres DA. Regulation of voltage-gated calcium channel activity by the Rem and Rad GTPases. Proceedings of the National Academy of Sciences of the United States of America. 2003; 100:14469–14474. [PubMed: 14623965]
31. Chen H, Puhl HL 3rd, Niu SL, Mitchell DC, Ikeda SR. Expression of Rem2, an RGK family small GTPase, reduces N-type calcium current without affecting channel surface density. J Neurosci. 2005; 25:9762–9772. [PubMed: 16237180]
32. Kelly K. The RGK family: a regulatory tail of small GTP-binding proteins. Trends Cell Biol. 2005; 15:640–643. [PubMed: 16242932]
33. Beguin P, Mahalakshmi RN, Nagashima K, Cher DH, Takahashi A, Yamada Y, et al. 14-3-3 and calmodulin control subcellular distribution of Kir/Gem and its regulation of cell shape and calcium channel activity. J Cell Sci. 2005; 118:1923–1934. [PubMed: 15860732]
34. Beguin P, Mahalakshmi RN, Nagashima K, Cher DH, Kuwamura N, Yamada Y, et al. Roles of 14-3-3 and calmodulin binding in subcellular localization and function of the small G-protein Rem2. Biochem J. 2005; 390:67–75. [PubMed: 15862114]
35. Beguin P, Mahalakshmi RN, Nagashima K, Cher DH, Ikeda H, Yamada Y, et al. Nuclear sequestration of beta-subunits by Rad and Rem is controlled by 14-3-3 and calmodulin and reveals a novel mechanism for Ca2+ channel regulation. J Mol Biol. 2006; 355:34–46. [PubMed: 16298391]
36. Zhu J, Reynet C, Caldwell JS, Kahn CR. Characterization of Rad, a new member of Ras/GTPase superfamily, and its regulation by a unique GTPase-activating protein (GAP)-like activity. J Biol Chem. 1995; 270:4805–4812. [PubMed: 7876254]

37. Splingard A, Menetrey J, Perderiset M, Cicolari J, Regazzoni K, Hamoudi F, et al. Biochemical and structural characterization of the gem GTPase. J Biol Chem. 2007; 282:1905–1915. [PubMed: 17107948]
38. Opatowsky Y, Sasson Y, Shaked I, Ward Y, Chomsky-Hecht O, Litvak Y, et al. Structure-function studies of the G-domain from human gem, a novel small G-protein. FEBS Lett. 2006; 580:5959–5964. [PubMed: 17052716]
39. Finlin BS, Mosley AL, Crump SM, Correll RN, Ozcan S, Satin J, et al. Regulation of L-type Ca2+ channel activity and insulin secretion by the Rem2 GTPase. J Biol Chem. 2005; 280:41864–41871. [PubMed: 15728182]
40. Beguin P, Nagashima K, Gonoi T, Shibasaki T, Takahashi K, Kashima Y, et al. Regulation of Ca2+ channel expression at the cell surface by the small G-protein kir/Gem. Nature. 2001; 411:701–706. [PubMed: 11395774]
41. Finlin BS, Correll RN, Pang C, Crump SM, Satin J, Andres DA. Analysis of the complex between Ca2+ channel beta-subunit and the Rem GTPase. J Biol Chem. 2006; 281:23557–23566. [PubMed: 16790445]
42. Crump SM, Correll RN, Schroder EA, Lester WC, Finlin BS, Andres DA, et al. L-type calcium channel alpha-subunit and protein kinase inhibitors modulate Rem-mediated regulation of current. Am J Physiol Heart Circ Physiol. 2006; 291:H1959–H1971. [PubMed: 16648185]
43. Seu L, Pitt GS. Dose-dependent and isoform-specific modulation of Ca2+ channels by RGK GTPases. J Gen Physiol. 2006; 128:605–613. [PubMed: 17074979]
44. Yada H, Murata M, Shimoda K, Yuasa S, Kawaguchi H, Ieda M, et al. Dominant negative suppression of Rad leads to QT prolongation and causes ventricular arrhythmias via modulation of L-type Ca2+ channels in the heart. Circulation research. 2007; 101:69–77. [PubMed: 17525370]
45. Beguin P, Ng YJ, Krause C, Mahalakshmi RN, Ng MY, Hunziker W. RGK small GTP-binding proteins interact with the nucleotide kinase domain of Ca2+-channel beta-subunits via an uncommon effector binding domain. J Biol Chem. 2007; 282:11509–11520. [PubMed: 17303572]
46. Dolphin AC. A short history of voltage-gated calcium channels. Br J Pharmacol. 2006; 147 Suppl 1:S56–S62. [PubMed: 16402121]
47. Hancock JF, Magee AI, Childs JE, Marshall CJ. All ras proteins are polyisoprenylated but only some are palmitoylated. Cell. 1989; 57:1167–1177. [PubMed: 2661017]
48. Willumsen BM, Norris K, Papageorge AG, Hubbert NL, Lowy DR. Harvey murine sarcoma virus p21 ras protein: biological and biochemical significance of the cysteine nearest the carboxy terminus. EMBO J. 1984; 3:2581–2585. [PubMed: 6096132]
49. Gutierrez L, Magee AI, Marshall CJ, Hancock JF. Post-translational processing of p21ras is two-step and involves carboxyl-methylation and carboxy-terminal proteolysis. EMBO J. 1989; 8:1093–1098. [PubMed: 2663468]
50. Correll RN, Pang C, Niedowicz DM, Satin J, Andres DA. Calmodulin binding is dispensable for Rem-mediated Ca2+ channel inhibition. Mol Cell Biochem. 2008; 310:103–110. [PubMed: 18057997]
51. Villalonga P, Lopez-Alcala C, Bosch M, Chiloeches A, Rocamora N, Gil J, et al. Calmodulin binds to K-Ras, but not to H- or N-Ras, and modulates its downstream signaling. Mol Cell Biol. 2001; 21:7345–7354. [PubMed: 11585916]
52. Plowman SJ, Hancock JF. Ras signaling from plasma membrane and endomembrane microdomains. Biochim Biophys Acta. 2005; 1746:274–283. [PubMed: 16039730]
53. de Leon M, Wang Y, Jones L, Perez-Reyes E, Wei X, Soong TW, et al. Essential Ca(2+)-binding motif for Ca(2+)-sensitive inactivation of L-type Ca2+ channels. Science. 1995; 270:1502–1506. [PubMed: 7491499]
54. Yang T, Suhail Y, Dalton S, Kernan T, Colecraft HM. Genetically encoded molecules for inducibly inactivating CaV channels. Nat Chem Biol. 2007; 3:795–804. [PubMed: 17952065]
55. Alseikhan BA, DeMaria CD, Colecraft HM, Yue DT. Engineered calmodulins reveal the unexpected eminence of Ca2+ channel inactivation in controlling heart excitation. Proceedings of the National Academy of Sciences of the United States of America. 2002; 99:17185–17190. [PubMed: 12486220]

56. Chang L, Zhang J, Tseng YH, Xie CQ, Ilany J, Bruning JC, et al. Rad GTPase deficiency leads to cardiac hypertrophy. Circulation. 2007; 116:2976–2983. [PubMed: 18056528]

57. Soldatov NM. Ca2+ channel moving tail: link between Ca2+-induced inactivation and Ca2+ signal transduction. Trends Pharmacol Sci. 2003; 24:167–171. [PubMed: 12707002]

58. Andres DA, Shao H, Crick DC, Finlin BS. Expression cloning of a novel farnesylated protein, RDJ2, encoding a DnaJ protein homologue. Arch Biochem Biophys. 1997; 346:113–124. [PubMed: 9328291]

59. Andres DA, Crump SM, Correll RN, Satin J, Finlin BS. Analyses of Rem/RGK Signaling and Biological Activity. Methods Enzymol. 2005; 407:484–498. [PubMed: 16757347]

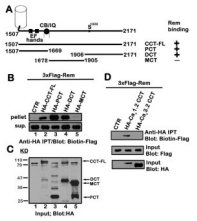

**Figure 1. Rem interacts with the proximal and distal domains of CCT**

*A*, Schematic of the CCT truncation mutants with the Rem interaction status indicated on the right. *B*, TsA201 cells were transiently co-transfected with expression vectors encoding 3xFlag-tagged Rem and either pCDNA3.1+3xHAa (empty vector), HA-CCT-FL or the indicated HA-tagged CCT truncation mutants. 48 h post-transfection, cells were harvested, and cell lysate (0.5 mg) was subjected to immunoprecipitation with anti-HA antibody as described under “Materials and Methods”. The entire bound fraction or a portion of the unbound fraction (2.5 μl) was analyzed by immunoblotting with biotin-Flag to detect Rem. *C*, Cell lysate (5 μg) was immunoblotted with anti-HA antibody to monitor expression of CCT-FL and the corresponding truncation mutants used in panel *B*. *D*, TsA201 cells were transiently co-transfected with vectors expressing Flag-Rem and either pCDNA3.1+3xHAa, HA-$Ca_V1.2$ CCT or HA-$Ca_V3.2$ CCT. Co-immunoprecipitation was performed using HA antibody as described in *B* and Rem binding examined by biotin-Flag immunoblotting. Results in each panel are representative of three independent experiments.

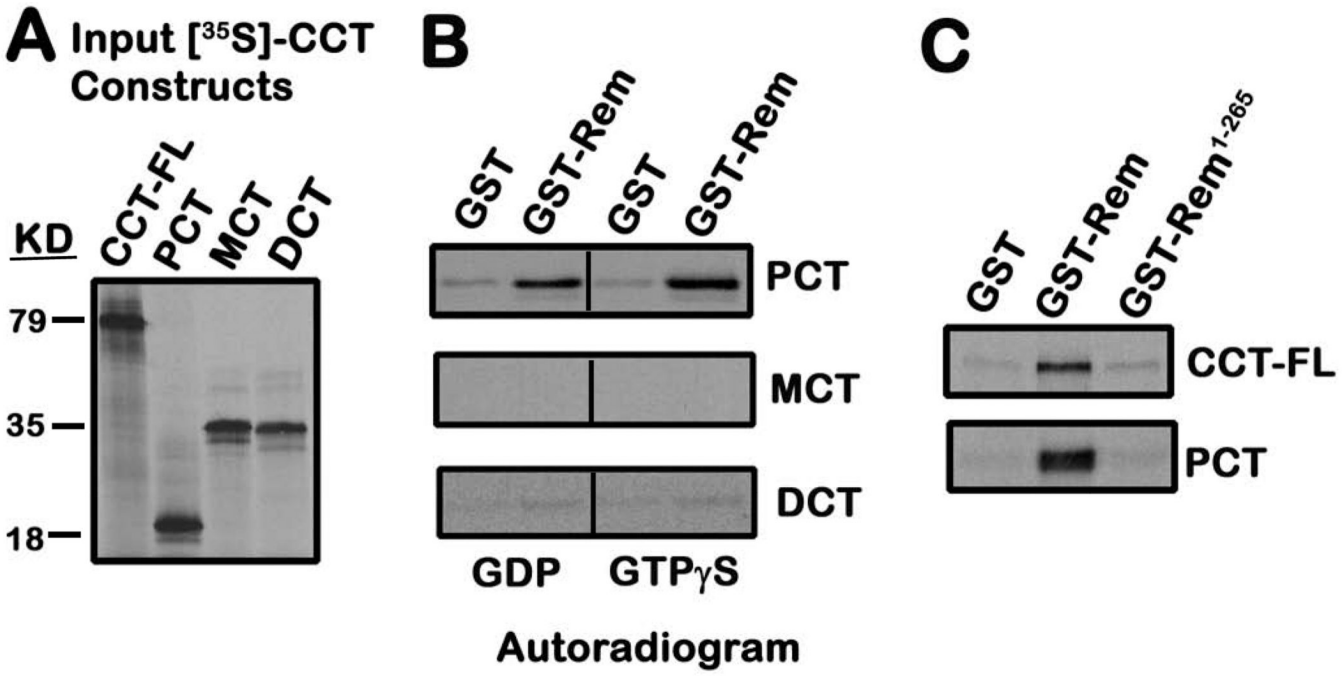


**Figure 2.** ***In vitro*** **association of Rem with proximal CCT**

*A*, $^{35}$S-labeled CCT truncation mutants were prepared by *in vitro* transcription and translation as described under "Materials and Methods". The $^{35}$S-labeled proteins were resolved on 10% SDS-PAGE, the gels dried and exposed to film for 3 h. *B*, Recombinant GST or GST-Rem proteins bound to glutathione-Sepharose resin were preloaded with the indicated nucleotide, and incubated with $^{35}$S-labeled CCT truncation mutants for 3h at 4°C. Bound proteins were resolved on SDS-PAGE, and the dried gel exposed to film for 16–72 h. Results are representative of four independent experiments. *C*, Recombinant GST, GST-Rem, or GST-Rem-(1-265) proteins were preloaded with GDP, bound to glutathione-Sepharose, and incubated with $^{35}$S-labeled CCT-FL or PCT (3 h at 4°C). The resin was pelleted, washed, and the bound fractions subjected to SDS-PAGE analysis. The dried gel was exposed to film for 24 h to detect bound CCT. Results are representative of three independent experiments.

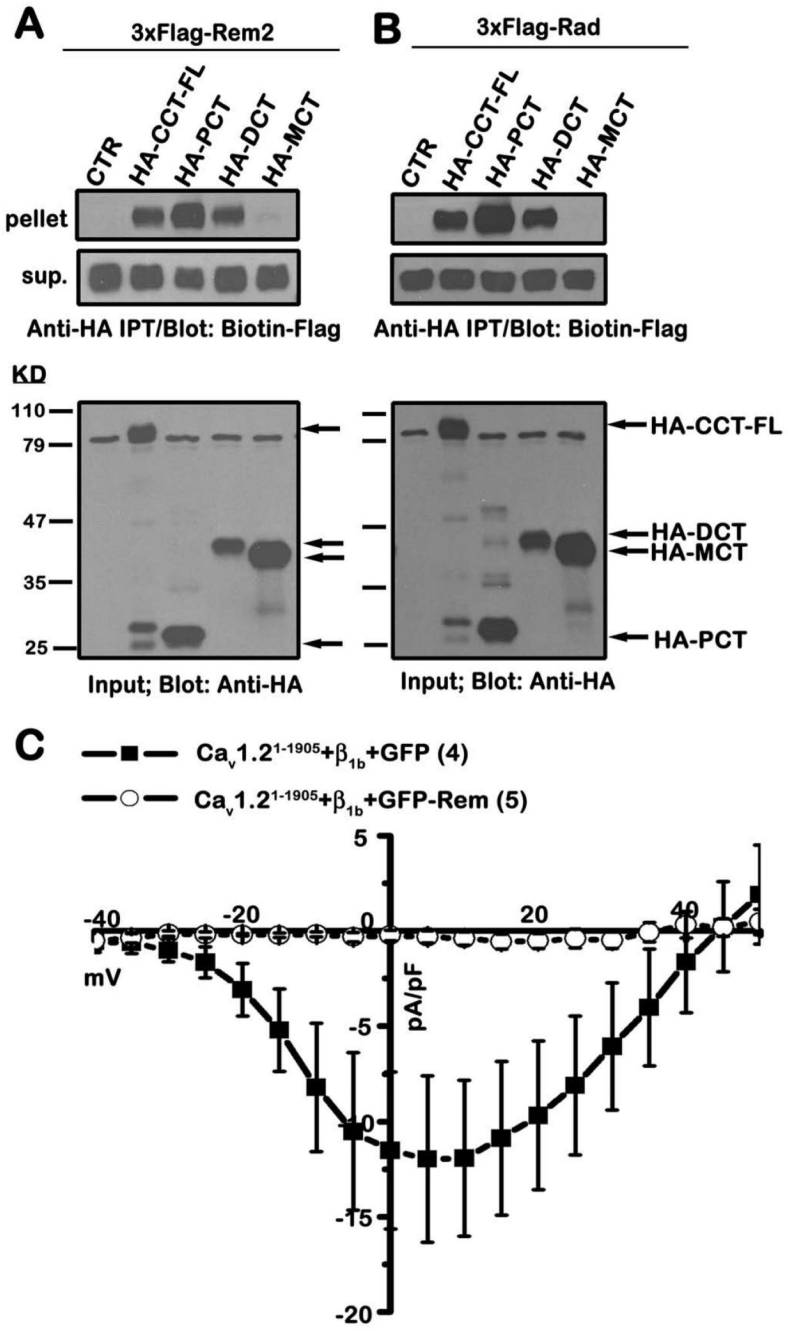


**Figure 3. Rem2 and Rad associate with the proximal and distal domains of CCT, but the distal domain is not required for $Ca^{2+}$ channel inhibition**

*A*, TsA201 cells were transiently co-transfected with expression vectors encoding 3xFlag-tagged Rem2 and either empty pCDNA3.1+3xHAa (control), HA-tagged CCT-FL or the indicated HA-tagged CCT truncation mutants. Co-immunoprecipitation was performed with anti-HA antibody and Rem2 binding examined by immunoblotting with biotinylated FLAG antibody. Results are representative of three independent experiments. *B*, TsA201 cells were transiently co-transfected with expression vectors encoding Flag-Rad and either HA-CCT-FL, the indicated HA-tagged CCT truncation mutants, or empty vector. Co-immunoprecipitation analysis was performed as described in *A*. Results are representative of

three independent experiments. *C*, TsA201 cells were transfected with plasmids expressing $Ca_v1.2(1–1905)$, $\beta_{1b}$ and either GFP-Rem or unfused GFP as control. Current was examined using the whole-cell patch clamp configuration in the presence of 30 mM $Ba^{2+}$.

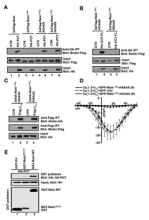

**Figure 4. Plasma membrane targeting is necessary for Rem:CCT association**

*A*, TsA201 cells were transiently co-transfected with the indicated Rem and CCT expression vectors. Co-immunoprecipitation was performed with anti-HA antibody and interaction with Rem examined by immunoblotting with biotinylated FLAG antibody. Results are representative of four independent experiments. *B*, TsA201 cells were transiently co-transfected with the indicated plasmids and co-immunoprecipitation performed with HA antibody as described in *A*. Results are representative of three independent experiments. *C*, TsA201 cells were transfected with the indicated plasmids. Co-immunoprecipitation was performed with Flag antibody and interaction with Rem proteins examined by immunoblotting with biotinylated anti-HA antibody. Immunoprecipitates were blotted for $\beta_{1b}$ using biotinylated Flag antibody. Results are representative of three independent experiments. *D*, TsA201 cells were transfected with plasmids expressing $Ca_V1.2$, $\beta_{1b}$ and either GFP-Rem-(1-265)-HCAAX, GFP-Rem-(1-265)-HSAAX, or unfused GFP as control. Current was examined using the whole-cell patch clamp configuration in the presence of 30 mM $Ba^{2+}$. *E*, TsA201 cells were transiently co-transfected with GST alone, GST-Rem, or GST-Rem(266–297) and PCT. GST fusion proteins were isolated using glutathione-Sepharose resin and interaction with PCT examined by immunoblotting. Results are representative of three independent experiments.

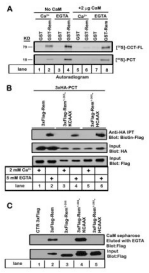

**Figure 5. $Ca^{2+}$/CaM inhibits *in vitro* Rem:CCT binding**

*A*, Recombinant GST or GST-Rem proteins bound to glutathione-Sepharose were preloaded with GDP, incubated for 3 h at 4°C with $^{35}$S-labeled CCT-FL (*top panel*) or PCT (*bottom panel*) in the presence of 2 mM $Ca^{2+}$ or 5 mM EGTA with or without CaM (2 μg). The glutathione-Sepharose beads were then pelleted and washed as described under "Materials and Methods". Bound proteins were subjected to SDS-PAGE, and the dried gel was exposed to film for 16–72 h. Results are representative of four independent experiments. *B*, TsA201 cells were transiently co-transfected with expression vectors encoding HA-PCT and Flag-Rem, Flag-Rem-(1-265)-KCAAX, or Flag-Rem-(1-265)-HCAAX. The ability of PCT to interact with either Rem or the indicated Rem chimeric proteins was determined by co-immunoprecipitation analysis as described under "Materials and Methods". Results are representative of three independent experiments. *C*, TsA201 cells were transfected with plasmids expressing 3xFlag-Rem, 3xFlag-Rem-(1-265), 3xFlag-Rem-(1-265)-KCAAX, 3xFlag-Rem-(1-265)-HCAAX or empty p3xFlag-CMV10 as control. Cell lysates (1 mg) were pulled down using CaM-sepharose beads in the presence of 2 mM $CaCl_2$, bound proteins were released with two washes with assay buffer (containing 5mM EGTA), and the ability to associate with CaM was examined by immunoblotting with anti-Flag antibody. Results are representative of three independent experiments.

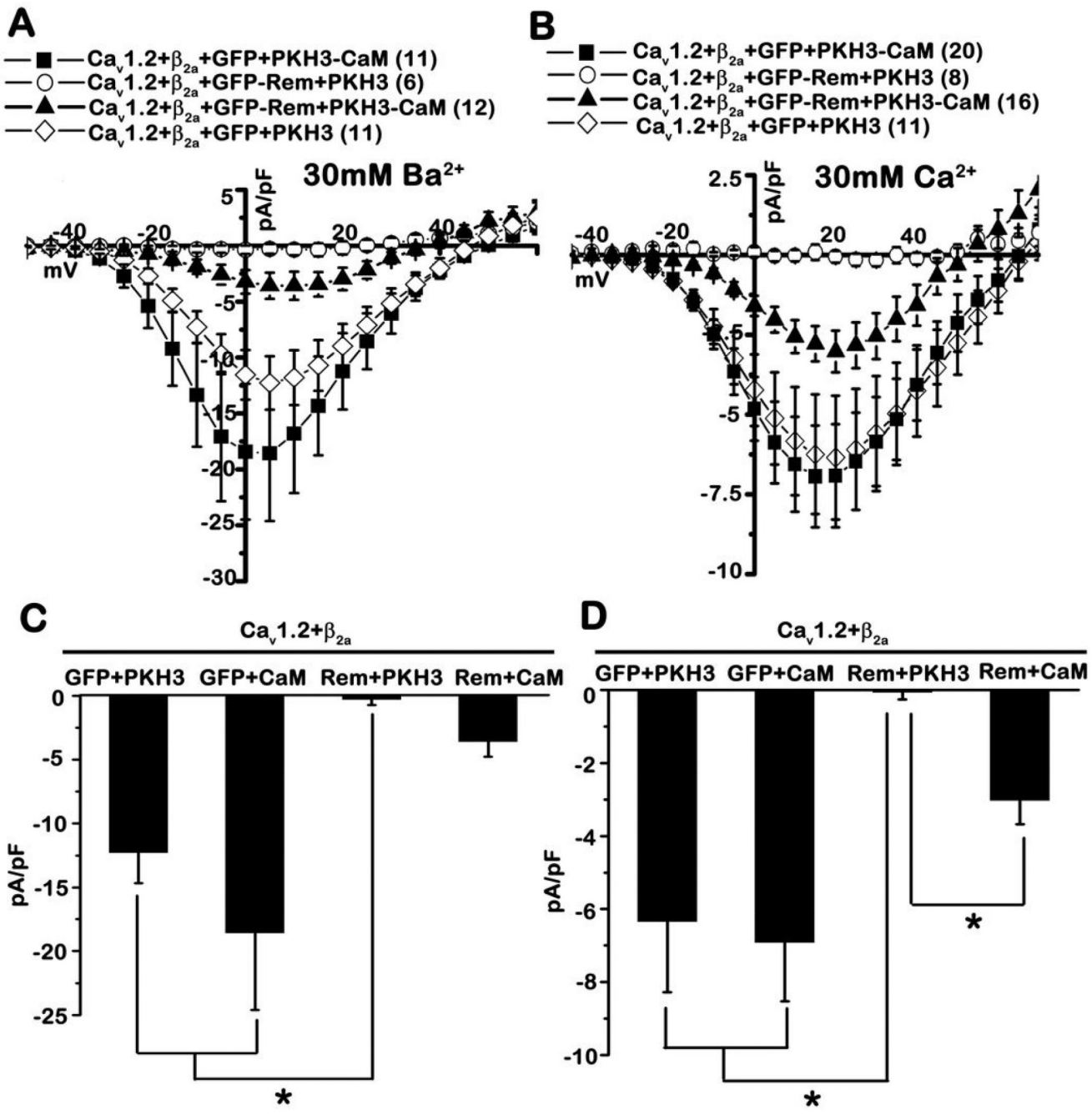


**Figure 6. Calmodulin expression blunts Rem-mediated $Ca^{2+}$ channel inhibition**

*A*, TsA201 cells were transfected with the indicated plasmids, and the current was examined in the presence of 30 mM $Ba^{2+}$ using the whole-cell patch clamp configuration. *B*, TsA201 cells were transfected as in panel *A*, and current was examined in the presence of 30 mM $Ca^{2+}$ using the whole-cell patch clamp configuration. *C*, Current density at +5 mV from *A*. *D*, Current density at +20 mV from panel *B*. A significant difference ($p<0.01$, Kruskal-Wallis test followed by a *post hoc* Dunn's test) between treatments is denoted by *asterisks*.

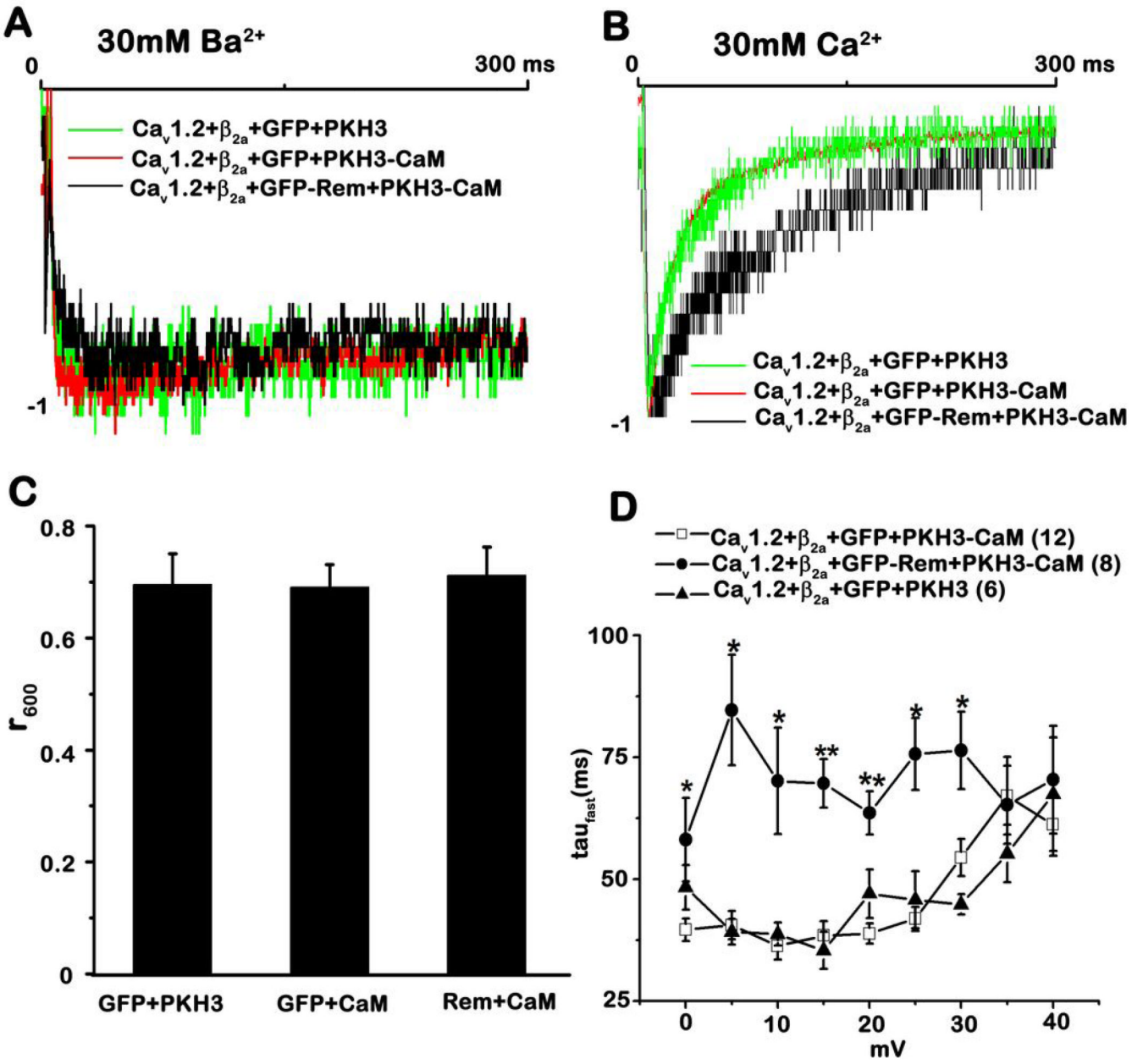


**Figure 7. Overexpression of Rem alters the kinetics of CDI**

*A*, Representative normalized $I_{Ba}$ traces recorded from tsA201 cells transfected with the indicated plasmids for $V_{test}$ +5 mV. *B*, Representative normalized $I_{Ca}$ traces recorded from tsA201 cells transfected with the indicated plasmids for $V_{test}$ +20 mV. *C*, Residual fraction of currents ($r_{600}$) remaining at the end of the test pulses for $V_{test}$ +5 mV in the presence of 30 mM $Ba^{2+}$. Note that there are no significant differences between conditions. *D*, Overexpression of Rem slows the inactivation kinetics of CDI. During an 800 ms test pulse to a series of depolarizing potentials ranging from 0 mV to 40 mV, the inactivation time constant tau was measured as described in "Materials and Methods" and the fast inactivation component $tau_{fast}$ plotted against the corresponding depolarizing potentials. The error bars represent the standard error of the mean. Analysis of the results by student's t test revealed a significant difference between treatments denoted by single ($P<0.05$) or double ($P<0.00005$)

*asterisks*. Statistical comparisons are between the transfection of $Ca_V1.2$+Flag-$\beta_{2a}$+GFP-Rem+pKH3-CaM (*filled circles*) and the transfection of $Ca_V1.2$+Flag-$\beta_{2a}$+GFP+pKH3-CaM (*open squares*).